



Geological Survey of Canada

CURRENT RESEARCH

2007-B6

---

**Grain-size distribution and gas  
permeability of sediment samples from the  
JPEX/JNOC/GSC et al. Mallik 5L-38 gas  
hydrate production research well,  
Northwest Territories**

---

*S. Connell-Madore and T.J. Katsube*

2007

CURRENT RESEARCH



Natural Resources  
Canada

Ressources naturelles  
Canada

Canada The logo of the Government of Canada, featuring a red maple leaf icon.

©Her Majesty the Queen in Right of Canada 2007

ISSN 1701-4387  
Catalogue No. M44-2007/B6E-PDF  
ISBN 978-0-662-47100-4

A copy of this publication is also available for reference in depository libraries across Canada through access to the Depository Services Program's Web site at <http://dsp-psd.pwgsc.gc.ca>

A free digital download of this publication is available from GeoPub:  
[http://geopub.nrcan.gc.ca/index\\_e.php](http://geopub.nrcan.gc.ca/index_e.php)

Toll-free (Canada and U.S.A.): 1-888-252-4301

**Critical reviewers**  
Barbara Medioli  
Dale Issler

**Authors**

S. Connell-Madore ([sconnell@nrcan.gc.ca](mailto:sconnell@nrcan.gc.ca))  
T.J. Katsube ([jkatsube@nrcan.gc.ca](mailto:jkatsube@nrcan.gc.ca))  
Geological Survey of Canada  
601 Booth Street  
Ottawa, Ontario K1A 0E8

Publication approved by GSC Northern Canada

Correction date:

All requests for permission to reproduce this work, in whole or in part, for purposes of commercial use, resale, or redistribution shall be addressed to:  
Data Dissemination Division, Room 290C, 601 Booth Street, Ottawa, Ontario  
K1A 0E8.

# **Grain-size distribution and gas permeability of sediment samples from the JPEX/JNOC/GSC et al. Mallik 5L-38 gas hydrate production research well, Northwest Territories**

S. Connell-Madore and T.J. Katsube

Connell-Madore, S. and Katsube, T.J., 2007: Grain-size distribution and gas permeability of sediment samples from the JPEX/JNOC/GSC et al. Mallik 5L-38 gas hydrate production research well, Northwest Territories; Geological Survey of Canada, Current Research 2007-B6, 13 p.

---

**Abstract:** Grain-size distribution and gas permeability ( $k_G$ ) have been determined for 28 sediment samples from a depth range of 908.05–1090.89 m in the JAPEX/JNOC/GSC et al. Mallik 5L-38 gas hydrate production research well in the Mackenzie-Beaufort Basin, Northwest Territories. The main purpose of this paper is to illustrate the relationship between gas permeability ( $k_G$ ) and grain-size distribution.

Sample grain-size distributions are unimodal to multimodal and  $k_G$  values are in the range of 0.12–6957 mD ( $\times 10^{-15} \text{ m}^2$ ). The relationship between  $k_G$  and the main mode ( $d_m$ ) of the grain-size distributions shows three distinct trends:  $k_G$  increases at a high rate (Group A), a moderate rate (Group B), and a low rate (Group C) with increasing  $d_m$ . These trends are considered to be closely related to the clay content of the samples.

**Résumé :** On a déterminé la granulométrie et la perméabilité aux gaz ( $k_G$ ) de 28 échantillons de sédiments prélevés à des profondeurs variant entre 908,05 et 1090,89 m, dans le puits de recherche sur la production d'hydrates de gaz JAPEX/JNOC/GSC et al. Mallik 5L-38, dans le bassin de Beaufort-Mackenzie, dans les Territoires du Nord-Ouest. Le présent article a pour principal objectif d'illustrer le lien entre la perméabilité aux gaz ( $k_G$ ) et la granulométrie.

La distribution granulométrique des échantillons varie d'unimodale à plurimodale et les valeurs de  $k_G$  se situent dans la plage de 0,12 à 6957 mD ( $\times 10^{-15} \text{ m}^2$ ). Le lien établi entre  $k_G$  et le mode de distribution granulométrique principal ( $d_m$ ) met en évidence trois tendances distinctes : dans le premier cas, la valeur de  $k_G$  augmente rapidement avec l'accroissement de  $d_m$  (groupe A), dans le deuxième, elle augmente à une vitesse moyenne (groupe B), et dans le troisième, elle augmente lentement (groupe C). On suppose que les tendances observées sont étroitement liées à la teneur en argile des échantillons.

## INTRODUCTION

Grain-size distribution analysis and gas permeability ( $k_G$ ) testing were performed on 28 sediment samples from the Mallik 5L-38 research well, Northwest Territories, Canada (Fig. 1). Samples were collected from a depth range of 908.05–1089.89 m (Table 1). This paper documents and discusses the relationship between the grain-size distribution and the  $k_G$  data, which has been only partially reported in some of the more generalized papers (e.g. Katsube et al., 2005; Winters et al., 2005; Connell-Madore and Katsube, 2007).

## METHOD OF INVESTIGATION

Two specimens from each of the 28 samples (Table 1) were prepared and sent to AGAT Laboratories (Calgary, Alberta) for the grain-size analysis and gas-permeability ( $k_G$ ) testing. Routine petrophysical techniques were used to measure  $k_G$  in accordance with the American Petroleum Institute's Recommended Practices for Core Analysis Procedure (American Petroleum Institute, 1960). Results of the  $k_G$  tests have been published previously (Katsube et al., 2005), and are listed in Table 1. Part of the grain-size data are available in a published database (Dallimore et al., 2005) and the complete data set is listed in Appendices A1 to A3 of this paper.

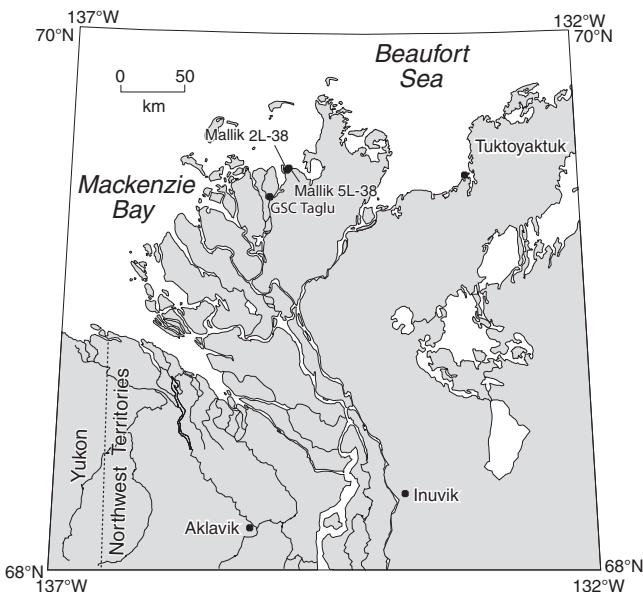


**Figure 1.** Map of the Mackenzie Delta region showing the location of the JAPEX/JNOC/GSC Mallik 2L-38 and JAPEX/JNOC/GSC et al. 5L-38 drill sites (Medioli et al., 2005).

## ANALYTICAL RESULTS

The complete grain-size distribution results for the 10 clayey silt samples are listed in Appendix A1 and those for the eighteen sandy samples are listed in Appendices A2 and A3.

The ten clayey silt samples (Fig. 2) display bimodal or multimodal asymmetric grain-size distribution patterns and have  $k_G$  values in the range of 0.12–2.85 mD (Table 1). The grain-size distributions for these samples have a main mode between clay and/or very fine silt (8.147–20.7  $\mu\text{m}$ ) and fine sand (146.8–213.2  $\mu\text{m}$ ), as shown in Figure 2. One of these clayey silt samples (P2EJA-20) displays a bimodal grain-size distribution with the main modes in the clay size range (18.86  $\mu\text{m}$ ) and in the silt size range (47.93  $\mu\text{m}$ ). The eighteen sandy samples (Fig. 3) also display asymmetrical grain-size distributions that are predominantly unimodal. The  $k_G$  values are in the range of 194–6957 mD (Table 1) and the main modes for these samples are in the very fine-grained to medium-grained sand size range (121.8–493.6  $\mu\text{m}$ ).

## DATA ANALYSIS

Gas permeability ( $k_G$ ) is plotted against the main grain-size modes ( $d_m$ ) in Figure 4. In this diagram three major trends are observed: one represented by Group A, displaying a rapid  $k_G$  increase with increased  $d_m$ ; a second represented by Group B, displaying a moderate  $k_G$  increase with increased  $d_m$ ; and a third represented by Group C, displaying a slow  $k_G$  increase with increased  $d_m$ .

The four Group A samples, displaying a very rapid  $k_G$  increase (1813–5209 mD) with increased  $d_m$  (161.2–194.2  $\mu\text{m}$ ) have very similar grain-size distributions (Fig. 5a). That is, their clay- and silt-size populations are substantially smaller (Tables 2 and 3) compared to samples in the other two groups, and their  $d_m$  values are almost identical.

The seven Group B samples, displaying a moderate  $k_G$  increase with increased  $d_m$ , can be divided into two subgroups, Subgroup Ba and Subgroup Bb. Subgroup Ba consists of five samples with almost identical grain-size distributions (Fig. 5b) and  $d_m$  values (256.8–339.8  $\mu\text{m}$ ). Their  $k_G$  values are in the range of 2464–4910 mD. The two Subgroup Bb samples (Fig. 5c) have a more complicated grain-size distribution. The  $d_m$  and  $k_G$  values are in the ranges of 373.1–493.6  $\mu\text{m}$  and 4062–6957 mD, respectively. Group B samples exhibit a slight bimodal grain-size distribution, whereas Group A samples are strongly unimodal. Subgroup Bb shows one minor mode at a grain size just above the  $d_m$  and another just below the  $d_m$ . Group Ba does not show any distinct minor modes, but shows a slightly lower differential volume increase in the vicinity of the 100  $\mu\text{m}$  grain-size range compared to that of the unimodal distributions of Group A. This could be considered a very minor bimodal distribution effect.

**Table 1.** Sample descriptions, gas permeability ( $k_g$ ) and main grain-size modes ( $d_m$ ) for the Mallik 5L-38 well listed in order of increasing depth.

Sample number	Depth (m)	Lithology	Gas permeability, $k_g$ (mD)	Main mode ( $d_m$ ) of the grain-size distribution ( $\mu\text{m}$ )
P2EJA-11	908.05	Fine sand	1419.00	Fine sand 234.10
P2EJA-26	910.61	Fine sand	4062.00	Medium sand 373.10
P2EJA-16	916.19	Fine sand	5209.00	Fine sand 194.20
P2EJA-17	918.95	Fine sand	4963.00	Fine sand 194.20
P2EJA-21	920.81	Fine sand	3687.00	Fine sand 176.80
P2EJA-27	925.09	Fine sand	1813.00	Fine sand 161.20
P2EJA-7	927.35	Fine sand	4910.00	Medium sand 339.80
P2EJA-25	933.58	Clayey silt	2.85	Fine sand 146.80
P2EJA-4	937.47	Clayey silt	1.55	Clayey silt 213.20
P2EJA-13	939.88	Clayey silt	0.43	Silt 20.70
P2EJA-19	953.47	Silty sand	236.00	Fine sand 146.80
P2EJA-2	955.69	Medium sand	6957.00	Medium sand 493.60
P2EJA-20	972.05	Clayey silt	2.15	Clayey silt 18.86, 47.93
P2EJA-14	973.08	Sand with organic material	1590.00	Medium sand 339.80
P2EJA-22	975.67	Silty sand	2464.00	Medium sand 282.10
P2EJA-5	980.65	Fine sand	3546.00	Medium sand 309.60
P2EJA-10	982.59	Clayey silt	0.37	Silt 20.70
P2EJA-28	987.53	Fine sand	1091.00	Fine sand 194.20
P2EJA-1	989.73	Fine sand	3257.00	Medium sand 282.10
P2EJA-8	1004.93	Clayey silt	0.12	Mud, fine sand 161.20
P2EJA-24	1022.42	Fine sand	1904.00	Medium sand 282.10
P2EJA-15	1028.78	Clayey silt	0.61	Clayey silt 18.86
P2EJA-9	1042.12	Clayey silt	0.54	Clayey silt 8.15
P2EJA-18	1063.47	Organic shale, clayey coal	0.43	Clayey silt 146.80
P2EJA-12	1072.75	Silty sand	194.00	Very fine sand 121.80
P2EJA-6	1076.63	Fine sand	2658.00	Medium sand 256.80
P2EJA-3	1083.45	Clayey silt	0.32	Clayey silt 18.86
P2EJA-23	1089.89	Fine sand	1430.00	Medium sand 282.10

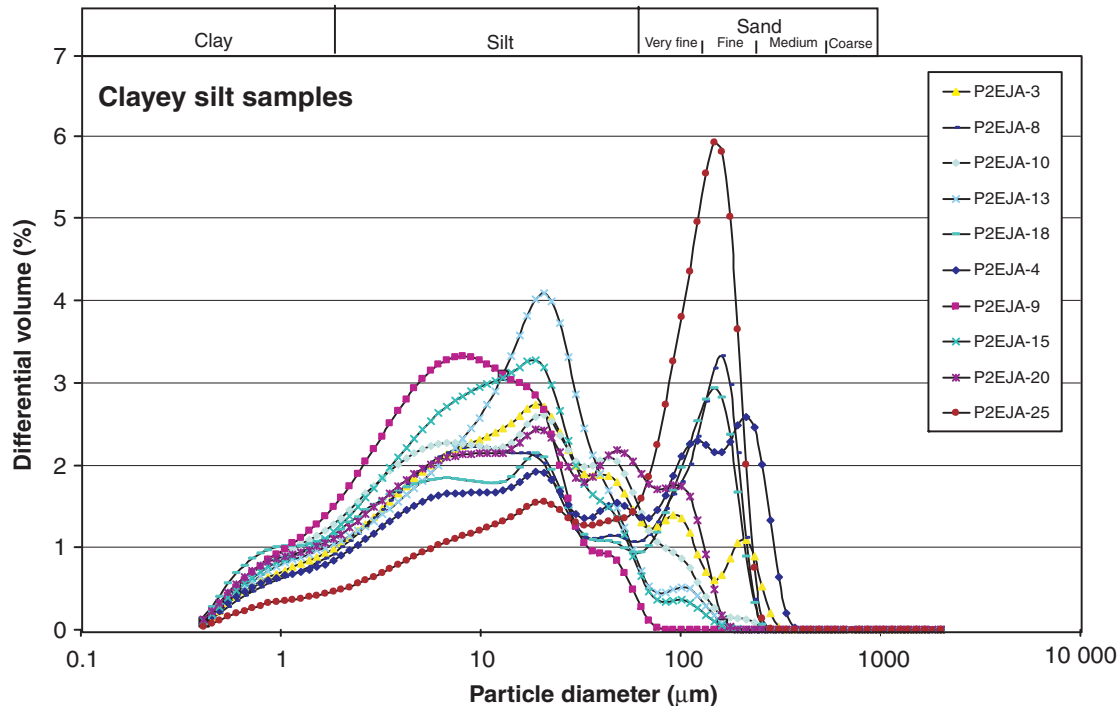


**Figure 2.** Grain-size distributions of ten clayey silt samples from the Mallik 5L-38 well, Northwest Territories.

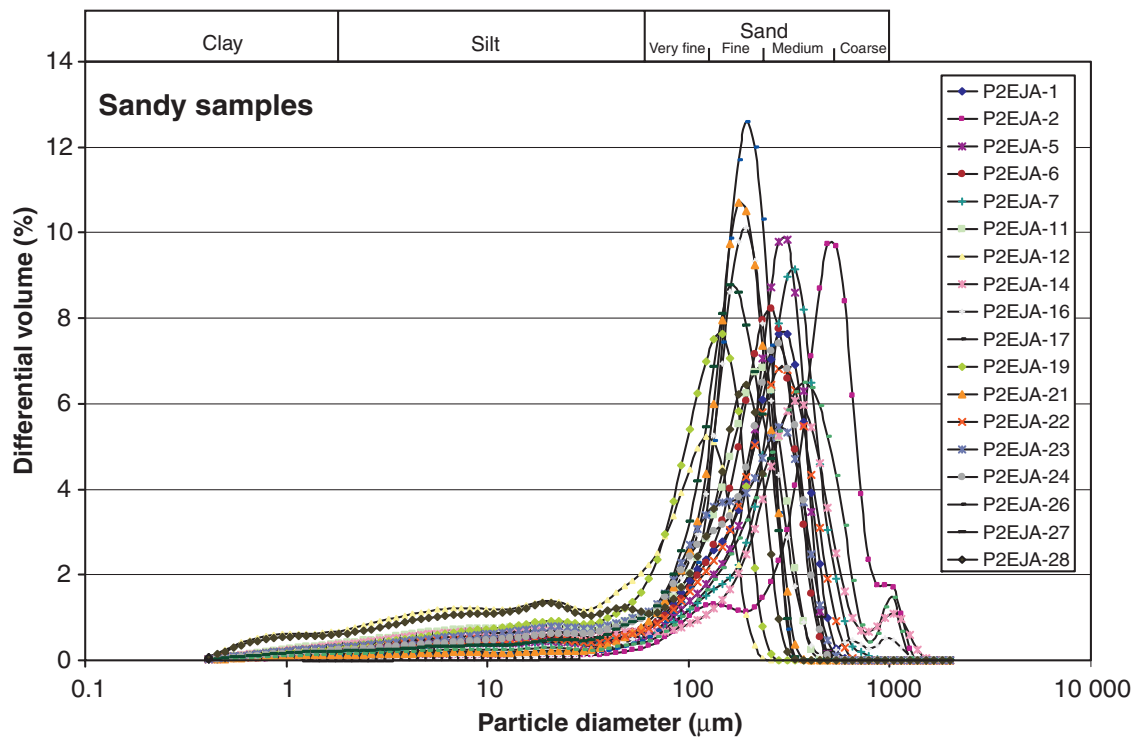


**Figure 3.** Grain-size distributions of eighteen sandy samples from the Mallik 5L-38 well, Northwest Territories.

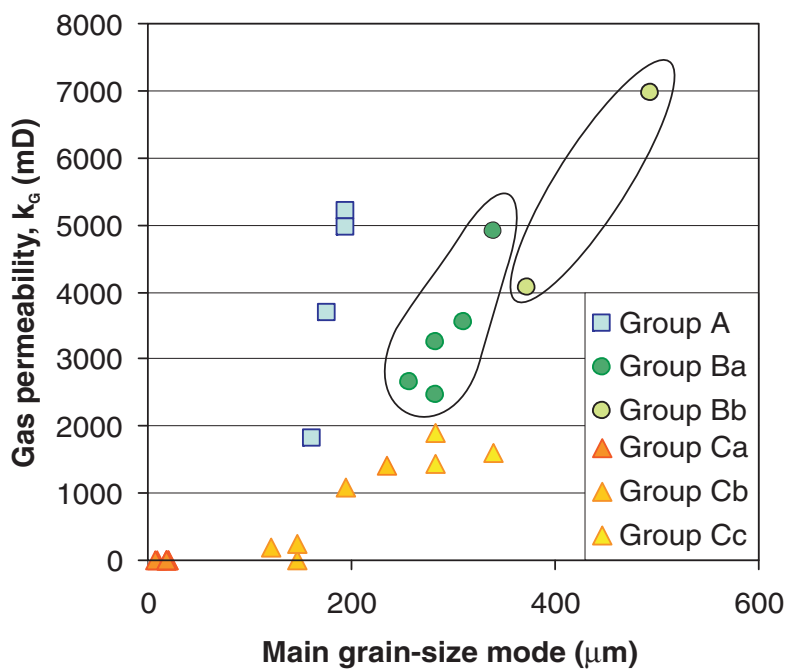


**Figure 4.** Gas permeability ( $k_g$ ) versus main grain-size mode ( $d_m$ ) for the 28 Mallik samples. Three main groups are identified: Group A, B, and C.

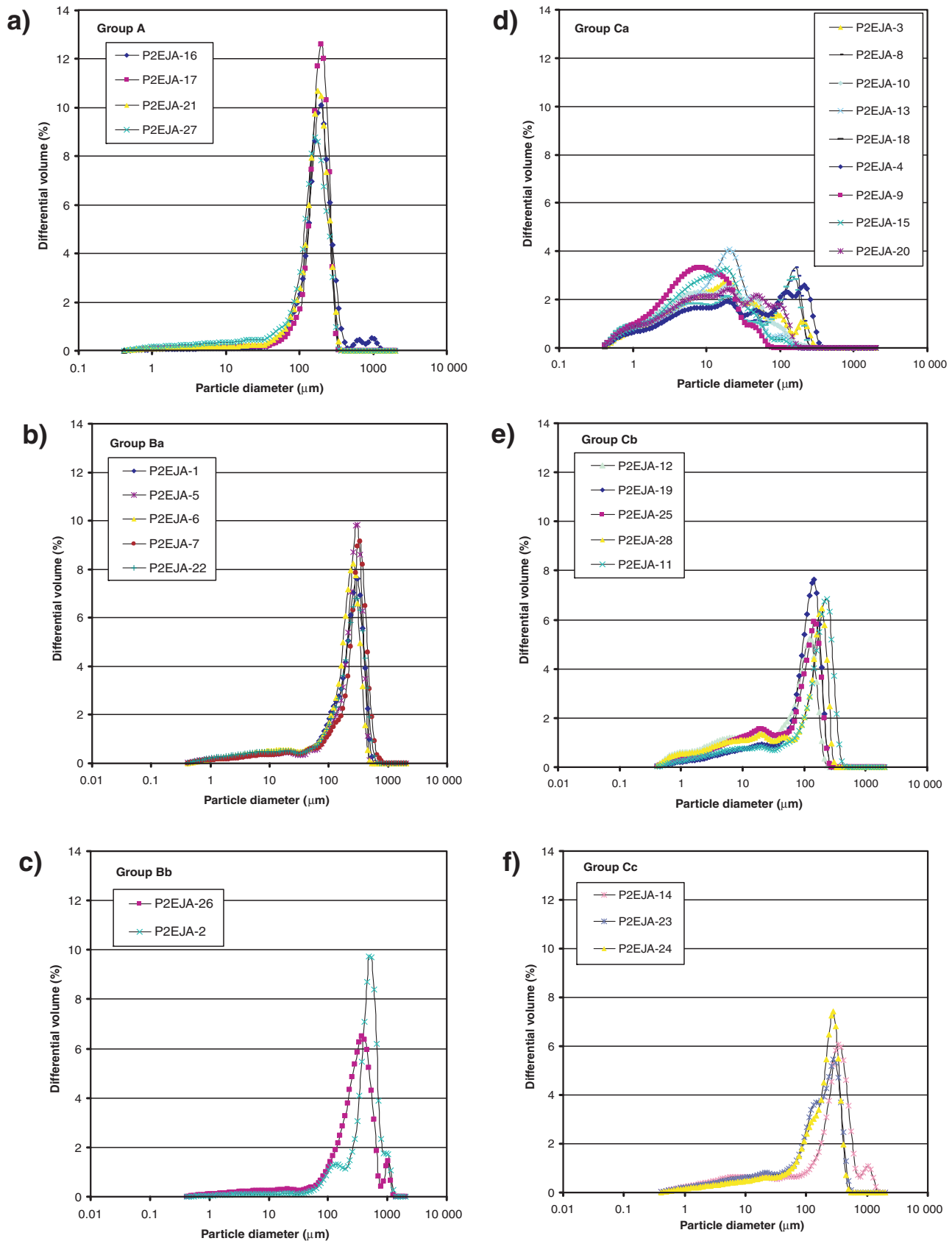


**Figure 5.** Grain-size distributions for samples of **a)** Group A, **b)** Subgroup Ba, **c)** Subgroup Bb, **d)** Subgroup Ca, **e)** Subgroup Cb, and **f)** Subgroup Cc.

**Table 2.** Volume percentages of the different grain-size ranges for the 28 samples from the Mallik 5L-38 well.

Sample number	Differential volume (%)							
	Clay <20 µm	Silt 20–62 µm	Very fine sand 62–125 µm	Fine sand 125–250 µm	Medium sand 250–500 µm	Coarse sand 500–1000 µm	Very coarse sand 1000–2000 µm	Total
P2EJA-1	12.50	5.91	12.04	27.27	41.96	0.32	0.00	100.00
P2EJA-2	3.44	1.81	6.39	8.86	42.32	34.05	3.10	99.97
P2EJA-3	61.83	21.57	9.97	5.87	0.77	0.00	0.00	100.01
P2EJA-4	48.55	16.56	14.35	16.37	4.21	0.00	0.00	100.04
P2EJA-5	11.73	4.72	9.02	26.53	47.98	0.00	0.00	99.98
P2EJA-6	13.59	6.05	11.32	36.18	32.86	0.01	0.00	100.01
P2EJA-7	9.95	5.21	7.95	18.80	54.65	3.45	0.00	100.01
P2EJA-8	57.40	13.88	12.80	15.87	0.06	0.00	0.00	100.01
P2EJA-9	86.53	13.07	0.41	0.00	0.00	0.00	0.00	100.01
P2EJA-10	67.94	22.87	7.83	1.34	0.05	0.00	0.00	100.02
P2EJA-11	20.91	8.94	14.03	37.52	18.59	0.00	0.00	99.99
P2EJA-12	37.53	16.14	29.54	16.79	0.00	0.00	0.00	100.00
P2EJA-13	69.66	25.71	4.07	0.56	0.00	0.00	0.00	99.99
P2EJA-14	18.72	6.82	6.32	15.64	41.26	8.28	2.94	99.98
P2EJA-15	76.71	19.79	3.13	0.38	0.00	0.00	0.00	100.01
P2EJA-16	3.23	2.93	15.85	57.94	16.53	2.65	0.90	100.03
P2EJA-17	4.78	2.68	11.96	69.03	11.53	0.00	0.00	99.98
P2EJA-18	17.10	9.20	17.33	27.67	41.20	1.27	0.00	100.00
P2EJA-19	19.22	11.49	34.10	35.03	0.15	0.00	0.00	99.99
P2EJA-20	62.39	22.45	13.55	1.63	0.00	0.00	0.00	100.02
P2EJA-21	6.02	4.25	17.39	61.49	10.80	0.00	0.00	99.95
P2EJA-22	14.56	5.52	10.67	26.78	46.35	12.41	2.17	100.00
P2EJA-23	59.36	13.80	12.99	13.81	0.06	0.00	0.00	100.02
P2EJA-24	13.01	7.91	15.71	29.84	33.52	0.01	0.00	100.00
P2EJA-25	31.47	14.91	24.80	28.70	0.15	0.00	0.00	100.03
P2EJA-26	7.29	3.24	7.79	20.75	46.35	12.41	2.17	100.00
P2EJA-27	10.47	6.81	21.36	52.64	8.76	0.00	0.00	100.04
P2EJA-28	33.52	12.75	13.94	36.19	3.65	0.00	0.00	100.04

**Table 3.** Volume percentages of the different grain-size ranges for the 28 samples listed by the groups (A, B, and C) defined in Figure 3.

Group and sample number	Differential volume (%)								
	Clay <20 µm	Silt 20–62 µm	Very fine sand 62–125 µm	Fine sand 125–250 µm	Medium sand 250–500 µm	Coarse sand 500–1000 µm	Very coarse sand 1000–2000 µm	Total	
A	P2EJA-16	3.23	2.93	15.85	57.94	16.53	2.65	0.90	100.03
	P2EJA-17	4.78	2.68	11.96	69.03	11.53	0.00	0.00	99.98
	P2EJA-21	6.02	4.25	17.39	61.49	10.80	0.00	0.00	99.95
	P2EJA-27	10.47	6.81	21.36	52.64	8.76	0.00	0.00	100.04
Ba	P2EJA-1	12.50	5.91	12.04	27.27	41.96	0.32	0.00	100.00
	P2EJA-5	11.73	4.72	9.02	26.53	47.98	0.00	0.00	99.98
	P2EJA-6	13.59	6.05	11.32	36.18	32.86	0.01	0.00	100.01
	P2EJA-7	9.95	5.21	7.95	18.80	54.65	3.45	0.00	100.01
	P2EJA-22	14.56	5.52	10.67	26.78	41.20	1.27	0.00	100.00
Bb	P2EJA-2	3.44	1.81	6.39	8.86	42.32	34.05	3.10	99.97
	P2EJA-26	7.29	3.24	7.79	20.75	46.35	12.41	2.17	100.00
Ca	P2EJA-3	61.83	21.57	9.97	5.87	0.77	0.00	0.00	100.01
	P2EJA-4	48.55	16.56	14.35	16.37	4.21	0.00	0.00	100.04
	P2EJA-8	57.40	13.88	12.80	15.87	0.06	0.00	0.00	100.01
	P2EJA-9	86.53	13.07	0.41	0.00	0.00	0.00	0.00	100.01
	P2EJA-10	67.94	22.87	7.83	1.34	0.05	0.00	0.00	100.02
	P2EJA-13	69.66	25.71	4.07	0.56	0.00	0.00	0.00	99.99
	P2EJA-15	76.71	19.79	3.13	0.38	0.00	0.00	0.00	100.01
	P2EJA-18	59.36	13.80	12.99	13.81	0.06	0.00	0.00	100.02
	P2EJA-20	62.39	22.45	13.55	1.63	0.00	0.00	0.00	100.02
	P2EJA-11	20.91	8.94	14.03	37.52	18.59	0.00	0.00	99.99
Cb	P2EJA-12	37.53	16.14	29.54	16.79	0.00	0.00	0.00	100.00
	P2EJA-19	19.22	11.49	34.10	35.03	0.15	0.00	0.00	99.99
	P2EJA-25	31.47	14.91	24.80	28.70	0.15	0.00	0.00	100.03
	P2EJA-28	33.52	12.75	13.94	36.19	3.65	0.00	0.00	100.04
	P2EJA-14	18.72	6.82	6.32	15.64	41.26	8.28	2.94	99.98
Cc	P2EJA-23	17.10	9.20	17.33	27.67	28.61	0.09	0.00	100.01
	P2EJA-24	13.01	7.91	15.71	29.84	33.52	0.01	0.00	100.00

Group C samples display a slow  $k_G$  increase with increased  $d_m$  representing samples with the highest clay and silt concentrations, and can be divided into three subgroups, Subgroup Ca, Subgroup Cb, and Subgroup Cc. The nine Subgroup Ca samples have the smallest  $k_G$  (0.12–2.15 mD) and  $d_m$  (8.147–161.2  $\mu\text{m}$ ) values. In Figure 5d, the grain-size distributions of each of these samples clearly depicts the high concentrations of clay and silt. The grain-size distributions for the five Subgroup Cb samples are displayed in Figure 5e. The  $k_G$  increase (2.85–1419 mD) with  $d_m$  (121.8–234.1  $\mu\text{m}$ ) for this subgroup is slightly larger than those for the other two in this group. These samples have a relatively high clay and silt size fraction with a large population of very fine- and fine-grained sand size grains. The three samples in Subgroup Cc have the largest  $k_G$  (1430–1904 mD) and  $d_m$  (282.1–339.8  $\mu\text{m}$ ) values of this group, and have a slightly more complicated grain-size distribution with more modes (Fig. 5f). The clay and silt size fractions are still relatively high, but not as high as for the other samples in this group.

## DISCUSSION AND CONCLUSIONS

Three distinct trends are seen between the gas permeability ( $k_G$ ) and main grain-size mode ( $d_m$ ) relationship, as shown in Figure 4. The first, a very rapid  $k_G$  increase with increased  $d_m$  (Group A), the second, a moderate  $k_G$  increase with increased  $d_m$  (Group B), and the third a slow  $k_G$  increase with increased  $d_m$  (Group C). Group A is also characterized by a strong unimodal grain-size distribution (Fig. 5a), whereas Group B is characterized by a bimodal grain-size distribution (Fig. 5c) or a unimodal grain-size distribution with indications of a very minor bimodal grain-size distribution (Fig. 5b). The slow  $k_G$  increase with increased  $d_m$  (Group C) is characterized by a minor to major increase in the silt and clay grain-size fractions as can be seen in Figures 5d, e, and f.

The existence of these three different trends between  $k_G$  and  $d_m$ , which show relationships to the three different types of grain-size distribution patterns, is significant. The three different grain-size distribution patterns, such as the unimodal distributions (Fig. 5a, b), bimodal distribution (Fig. 5c), and multimodal and approximate multimodal distributions (Fig. 5d, e f), suggest different grain-size combinations. The fact that these distribution patterns are related to the  $k_G$ - $d_m$  relationships may imply that they control these relationships. There is a critical clay content (CCC) concept, related to hydrocarbon seal-quality prediction in sediments, that is currently in the stage of development. One of the suggestions proposed by that concept is that different framework grain-size combinations results in different intergranular pore spaces, or porosities. This implies that a certain clay content rate of increase will have a different pore-space-filling rate for different pore-size combinations, and could imply different  $k_G$ - $d_m$  relationships. Therefore, these relationships between the  $k_G$ - $d_m$  trends and the grain-size distribution

patterns could be of significance to the critical clay content concept development. Details of this concept is expected to be published in the near future.

The  $k_G$  increase with increased  $d_m$  (Fig. 4) is likely due to an increased interconnected pore diameter with increased  $d_m$ . It is commonly accepted that permeability increases are very sensitive to increases in connecting pore diameters (e.g. Freeze and Cherry, 1979; Walsh and Brace, 1984). The existence of these distinct  $k_G$  versus  $d_m$  or grain-size relationships may be providing information on the critical clay content (CCC) which is related to the hydrocarbon seal quality.

## ACKNOWLEDGMENTS

The authors are grateful to D. Issler (GSC Calgary) and B. Medioli (GSC Ottawa) for critically reviewing this paper and to AGAT Laboratories (Calgary, Alberta) for performing the grain-size analysis and gas-permeability testing. The authors would also like to acknowledge F. Wright (GSC Pacific) for his advice and support related to this study.

## REFERENCES

- American Petroleum Institute (API)**  
1960: Recommended practices for core-analysis procedure; API Recommended Practice 40 (RP 40), American Petroleum Institute, Washington, D.C., p. 55 (first edition).
- Connell-Madore, S. and Katsube, T.J.**  
2007: Pore-size distribution of samples from the Mallik 5L-38 well, Northwest Territories; Geological Survey of Canada, Current Research 2007-B2, 11 p.
- Dallimore, S.R., Medioli, B.E., Laframboise, R.R., and Giroux, D. (comp.)**  
2005: Mallik 2002 Gas Hydrate Production Research Well Program, Mackenzie Delta, Northwest Territories: well data and interactive data viewer; Appendix A in Scientific Results from the Mallik 2002 Gas Hydrate Production Research Well Program, Mackenzie Delta, Northwest Territories, Canada, (ed.) S.R. Dallimore and T.S. Collett; Geological Survey of Canada, Bulletin 585.
- Freeze, R.A. and Cherry, J.A.**  
1979: Groundwater; Prentice Hall, Upper Saddle River, New Jersey, 604 p.
- Katsube, T.J., Dallimore, S.R., Jonnasson, I.R., Connell-Madore, S., Medioli, B.E., Uchida, T., Wright, J.F., and Scromeda, N.**  
2005: Petrophysical characteristics of gas-hydrate-bearing and gas-hydrate-free formations in the JAPEX/JNOC/GSC et al Mallik 5L-38 gas hydrate production research well; in Scientific Results from the Mallik 2002 Gas Hydrate Production Research Well Program, Mackenzie Delta, Northwest Territories, Canada, (ed.) S.R. Dallimore and T.S. Collett; Geological Survey of Canada, Bulletin 585, 14 p.

- Medioli, B.E., Wilson, N., Dallimore, S.R., Paré, D., Brennan-Alpert, P., and Oda, H.**
- 2005: Sedimentology of the cored interval, JAPEX/JNOC/GSC et al. Mallik 5L-38 gas hydrate production research well; *in* Scientific Results from the Mallik 2002 Gas Hydrate Production Research Well Program, Mackenzie Delta, Northwest Territories, Canada, (ed.) S.R. Dallimore and T.S. Collett; Geological Survey of Canada, Bulletin 585, 21 p.
- Walsh, J.B. and Brace, W.F.**
- 1984: The effect of pressure on porosity and the transport properties of rocks; *Journal of Geophysical Research*, v. 89, p. 9425–9431.

- Winters, W.J., Dallimore, S.R., Collett, T.S., Medioli, B.E., Matsumoto, R., Katsube, T.J., and Brennan-Alpert, P.**
- 2005: Relationships of sediment physical properties from the JAPEX/JNOC/GSC et al., Mallik 5L-38 gas hydrate production research well; *in* Scientific Results from the Mallik 2002 Gas Hydrate Production Research Well Program, Mackenzie Delta, Northwest Territories, Canada, (ed.) S.R. Dallimore and T.S. Collett; Geological Survey of Canada, Bulletin 585, 9 p.

Geological Survey of Canada Project X83

## Appendix A1

### Particle-size analysis of ten clayey-silt samples (differential volume per cent).

Particle diameter ( $\mu\text{m}$ )	P2EJA-3	P2EJA-4	P2EJA-8	P2EJA-9	P2EJA-10	P2EJA-13	P2EJA-15	P2EJA-18	P2EJA-20	P2EJA-25
0.412	0.09	0.09	0.08	0.11	0.12	0.10	0.11	0.16	0.12	0.04
0.452	0.15	0.16	0.14	0.20	0.22	0.17	0.19	0.28	0.22	0.08
0.496	0.22	0.23	0.20	0.29	0.31	0.25	0.27	0.40	0.32	0.11
0.545	0.32	0.32	0.28	0.41	0.44	0.35	0.39	0.56	0.45	0.16
0.598	0.40	0.40	0.35	0.51	0.55	0.44	0.48	0.69	0.55	0.20
0.657	0.46	0.46	0.41	0.60	0.64	0.52	0.56	0.78	0.64	0.23
0.721	0.53	0.51	0.47	0.69	0.72	0.59	0.63	0.86	0.71	0.26
0.791	0.59	0.56	0.52	0.77	0.79	0.65	0.70	0.93	0.78	0.29
0.869	0.64	0.60	0.57	0.85	0.86	0.71	0.76	0.97	0.83	0.32
0.953	0.68	0.63	0.60	0.92	0.91	0.76	0.81	1.00	0.87	0.34
1.047	0.72	0.66	0.64	0.98	0.95	0.81	0.85	1.01	0.89	0.35
1.149	0.76	0.68	0.68	1.05	0.99	0.85	0.89	1.01	0.92	0.37
1.261	0.80	0.70	0.72	1.12	1.04	0.88	0.94	1.02	0.94	0.38
1.385	0.84	0.73	0.76	1.20	1.09	0.92	0.99	1.04	0.97	0.40
1.520	0.88	0.76	0.81	1.28	1.14	0.96	1.05	1.07	1.01	0.42
1.669	0.93	0.79	0.86	1.38	1.20	0.99	1.11	1.10	1.05	0.44
1.832	0.98	0.84	0.92	1.49	1.28	1.04	1.19	1.16	1.10	0.46
2.010	1.05	0.90	1.00	1.61	1.36	1.08	1.28	1.22	1.16	0.49
2.207	1.12	0.96	1.08	1.75	1.46	1.14	1.38	1.30	1.24	0.52
2.423	1.20	1.03	1.17	1.89	1.55	1.20	1.49	1.37	1.32	0.56
2.660	1.28	1.10	1.26	2.04	1.65	1.26	1.60	1.45	1.40	0.60
2.920	1.37	1.17	1.36	2.19	1.74	1.32	1.72	1.52	1.49	0.64
3.206	1.47	1.25	1.46	2.35	1.84	1.40	1.85	1.58	1.57	0.69
3.519	1.56	1.32	1.57	2.51	1.93	1.47	1.97	1.64	1.66	0.74
3.862	1.66	1.39	1.67	2.66	2.01	1.55	2.09	1.69	1.74	0.79
4.241	1.75	1.45	1.77	2.80	2.08	1.64	2.21	1.73	1.82	0.84
4.656	1.84	1.51	1.87	2.94	2.14	1.72	2.32	1.77	1.89	0.89
5.111	1.92	1.56	1.95	3.05	2.19	1.81	2.43	1.80	1.96	0.94
5.611	2.00	1.60	2.03	3.15	2.23	1.91	2.54	1.82	2.01	0.98
6.158	2.07	1.63	2.09	3.23	2.26	2.00	2.63	1.83	2.06	1.03
6.761	2.13	1.65	2.15	3.28	2.27	2.10	2.71	1.84	2.09	1.07
7.421	2.19	1.66	2.18	3.31	2.27	2.21	2.78	1.83	2.11	1.10
8.147	2.23	1.66	2.21	3.32	2.26	2.32	2.84	1.82	2.13	1.14
8.944	2.27	1.67	2.22	3.31	2.25	2.44	2.90	1.81	2.13	1.17
9.819	2.31	1.67	2.22	3.28	2.23	2.57	2.95	1.80	2.14	1.21
10.780	2.35	1.67	2.21	3.23	2.21	2.73	2.99	1.78	2.14	1.24
11.830	2.39	1.67	2.18	3.17	2.20	2.90	3.02	1.78	2.14	1.28
12.990	2.45	1.69	2.16	3.10	2.22	3.10	3.06	1.80	2.15	1.32
14.260	2.51	1.73	2.15	3.04	2.27	3.32	3.12	1.86	2.19	1.37
15.650	2.60	1.79	2.15	3.00	2.37	3.57	3.19	1.97	2.27	1.43
17.180	2.68	1.87	2.15	2.95	2.50	3.81	3.26	2.07	2.36	1.49
18.860	2.73	1.92	2.11	2.85	2.59	4.01	3.27	2.14	2.43	1.54
20.700	2.71	1.91	2.02	2.67	2.61	4.09	3.19	2.10	2.42	1.55
22.730	2.59	1.82	1.85	2.37	2.53	3.99	2.97	1.95	2.33	1.52
24.950	2.39	1.68	1.62	1.99	2.36	3.72	2.66	1.72	2.16	1.45
27.380	2.18	1.52	1.40	1.59	2.18	3.31	2.30	1.48	1.98	1.36
30.070	2.00	1.40	1.22	1.26	2.04	2.86	1.99	1.27	1.84	1.30
33.000	1.89	1.35	1.12	1.05	1.98	2.45	1.77	1.15	1.80	1.27

Particle diameter ( $\mu\text{m}$ )	P2EJA-3	P2EJA-4	P2EJA-8	P2EJA-9	P2EJA-10	P2EJA-13	P2EJA-15	P2EJA-18	P2EJA-20	P2EJA-25
36.240	1.87	1.37	1.10	0.95	2.00	2.12	1.64	1.09	1.86	1.27
39.770	1.88	1.44	1.12	0.93	2.06	1.89	1.57	1.08	1.99	1.29
43.660	1.87	1.51	1.14	0.91	2.10	1.69	1.49	1.08	2.12	1.32
47.930	1.79	1.54	1.14	0.84	2.05	1.48	1.36	1.05	2.18	1.34
52.630	1.65	1.50	1.10	0.69	1.90	1.24	1.15	0.99	2.15	1.36
57.770	1.46	1.43	1.07	0.49	1.67	0.96	0.89	0.94	2.04	1.43
63.410	1.31	1.37	1.08	0.27	1.42	0.71	0.65	0.94	1.89	1.59
69.620	1.23	1.36	1.16	0.11	1.21	0.53	0.47	1.02	1.77	1.86
76.430	1.25	1.45	1.30	0.03	1.07	0.45	0.37	1.18	1.71	2.25
83.900	1.33	1.63	1.47	0.00	0.99	0.45	0.34	1.42	1.72	2.74
92.090	1.39	1.87	1.64	0.00	0.94	0.49	0.35	1.69	1.76	3.26
101.100	1.36	2.11	1.80	0.00	0.87	0.52	0.36	1.97	1.75	3.80
111.000	1.18	2.26	2.01	0.00	0.75	0.50	0.33	2.24	1.62	4.35
121.800	0.92	2.30	2.34	0.00	0.58	0.42	0.26	2.53	1.33	4.95
133.700	0.70	2.24	2.77	0.00	0.40	0.29	0.18	2.80	0.92	5.54
146.800	0.60	2.16	3.18	0.00	0.26	0.17	0.10	2.94	0.49	5.92
161.200	0.67	2.16	3.32	0.00	0.18	0.07	0.06	2.82	0.18	5.81
176.800	0.86	2.28	2.97	0.00	0.15	0.02	0.03	2.37	0.03	5.02
194.200	1.06	2.48	2.14	0.00	0.14	0.00	0.01	1.67	0.00	3.65
213.200	1.09	2.59	1.12	0.00	0.12	0.00	0.00	0.89	0.00	2.01
234.100	0.89	2.46	0.37	0.00	0.09	0.00	0.00	0.32	0.00	0.75
256.800	0.53	2.01	0.06	0.00	0.04	0.00	0.00	0.06	0.00	0.14
282.100	0.20	1.33	0.00	0.00	0.01	0.00	0.00	0.00	0.00	0.01
309.600	0.04	0.64	0.00	0.00	0.00	0.00	0.00	0.00	0.00	0.00
339.800	0.00	0.20	0.00	0.00	0.00	0.00	0.00	0.00	0.00	0.00
373.100	0.00	0.03	0.00	0.00	0.00	0.00	0.00	0.00	0.00	0.00
409.600	0.00	0.00	0.00	0.00	0.00	0.00	0.00	0.00	0.00	0.00
449.700	0.00	0.00	0.00	0.00	0.00	0.00	0.00	0.00	0.00	0.00
493.600	0.00	0.00	0.00	0.00	0.00	0.00	0.00	0.00	0.00	0.00
541.900	0.00	0.00	0.00	0.00	0.00	0.00	0.00	0.00	0.00	0.00
594.900	0.00	0.00	0.00	0.00	0.00	0.00	0.00	0.00	0.00	0.00
653.000	0.00	0.00	0.00	0.00	0.00	0.00	0.00	0.00	0.00	0.00
716.900	0.00	0.00	0.00	0.00	0.00	0.00	0.00	0.00	0.00	0.00
786.900	0.00	0.00	0.00	0.00	0.00	0.00	0.00	0.00	0.00	0.00
863.900	0.00	0.00	0.00	0.00	0.00	0.00	0.00	0.00	0.00	0.00
948.200	0.00	0.00	0.00	0.00	0.00	0.00	0.00	0.00	0.00	0.00
1041.000	0.00	0.00	0.00	0.00	0.00	0.00	0.00	0.00	0.00	0.00
1143.000	0.00	0.00	0.00	0.00	0.00	0.00	0.00	0.00	0.00	0.00
1255.000	0.00	0.00	0.00	0.00	0.00	0.00	0.00	0.00	0.00	0.00
1377.000	0.00	0.00	0.00	0.00	0.00	0.00	0.00	0.00	0.00	0.00
1512.000	0.00	0.00	0.00	0.00	0.00	0.00	0.00	0.00	0.00	0.00
1660.000	0.00	0.00	0.00	0.00	0.00	0.00	0.00	0.00	0.00	0.00
1822.000	0.00	0.00	0.00	0.00	0.00	0.00	0.00	0.00	0.00	0.00
2000.000	0.00	0.00	0.00	0.00	0.00	0.00	0.00	0.00	0.00	0.00

## Appendix A2

**Particle-size analysis of ten sandy samples (differential volume per cent).**

<b>Particle diameter (<math>\mu\text{m}</math>)</b>	<b>P2EJA-1</b>	<b>P2EJA-2</b>	<b>P2EJA-5</b>	<b>P2EJA-6</b>	<b>P2EJA-7</b>	<b>P2EJA-11</b>	<b>P2EJA-12</b>	<b>P2EJA-14</b>	<b>P2EJA-16</b>	<b>P2EJA-17</b>
0.412	0.02	0.00	0.02	0.02	0.01	0.03	0.09	0.02	0.00	0.01
0.452	0.03	0.01	0.03	0.03	0.05	0.16	0.04	0.01	0.02	
0.496	0.04	0.01	0.06	0.05	0.05	0.24	0.06	0.02	0.03	
0.545	0.06	0.02	0.08	0.07	0.06	0.33	0.09	0.02	0.04	
0.598	0.08	0.02	0.10	0.08	0.08	0.41	0.12	0.03	0.04	
0.657	0.09	0.02	0.12	0.10	0.09	0.47	0.14	0.03	0.05	
0.721	0.11	0.03	0.14	0.11	0.11	0.52	0.16	0.04	0.06	
0.791	0.12	0.03	0.15	0.13	0.12	0.56	0.18	0.04	0.07	
0.869	0.14	0.04	0.17	0.15	0.13	0.59	0.21	0.05	0.08	
0.953	0.15	0.04	0.18	0.16	0.14	0.61	0.23	0.05	0.08	
1.047	0.17	0.05	0.19	0.17	0.15	0.61	0.25	0.06	0.09	
1.149	0.18	0.05	0.20	0.19	0.15	0.62	0.26	0.06	0.09	
1.261	0.19	0.06	0.20	0.20	0.16	0.62	0.28	0.07	0.10	
1.385	0.20	0.06	0.21	0.21	0.16	0.63	0.30	0.07	0.10	
1.520	0.22	0.07	0.21	0.22	0.17	0.64	0.32	0.07	0.10	
1.669	0.23	0.07	0.22	0.23	0.17	0.66	0.34	0.08	0.11	
1.832	0.24	0.07	0.22	0.25	0.18	0.68	0.36	0.08	0.11	
2.010	0.25	0.08	0.23	0.26	0.18	0.72	0.38	0.08	0.11	
2.207	0.26	0.08	0.24	0.27	0.19	0.76	0.40	0.08	0.11	
2.423	0.27	0.09	0.25	0.28	0.20	0.81	0.42	0.08	0.11	
2.660	0.29	0.09	0.26	0.30	0.20	0.86	0.44	0.08	0.11	
2.920	0.30	0.09	0.27	0.31	0.22	0.91	0.47	0.09	0.12	
3.206	0.31	0.10	0.29	0.33	0.23	0.96	0.49	0.09	0.12	
3.519	0.32	0.10	0.30	0.34	0.24	1.00	0.52	0.09	0.12	
3.862	0.34	0.10	0.32	0.36	0.26	1.05	0.54	0.09	0.12	
4.241	0.35	0.11	0.34	0.38	0.27	1.09	0.57	0.09	0.13	
4.656	0.36	0.11	0.35	0.39	0.29	1.12	0.59	0.09	0.13	
5.111	0.38	0.11	0.37	0.41	0.30	1.15	0.61	0.09	0.13	
5.611	0.39	0.11	0.38	0.43	0.31	1.18	0.63	0.09	0.14	
6.158	0.40	0.11	0.39	0.44	0.32	1.20	0.64	0.09	0.14	
6.761	0.41	0.11	0.39	0.46	0.33	1.21	0.65	0.09	0.14	
7.421	0.42	0.11	0.39	0.47	0.33	1.21	0.66	0.09	0.15	
8.147	0.43	0.11	0.39	0.49	0.34	1.21	0.66	0.09	0.15	
8.944	0.44	0.11	0.39	0.50	0.34	1.21	0.66	0.09	0.15	
9.819	0.44	0.11	0.39	0.51	0.35	1.20	0.66	0.10	0.15	
10.780	0.45	0.11	0.39	0.52	0.35	1.20	0.65	0.10	0.15	
11.830	0.46	0.11	0.39	0.52	0.35	1.19	0.65	0.10	0.15	
12.990	0.47	0.12	0.39	0.53	0.36	1.20	0.65	0.10	0.15	
14.260	0.48	0.12	0.40	0.54	0.37	1.23	0.65	0.10	0.15	
15.650	0.49	0.12	0.41	0.54	0.39	1.28	0.67	0.11	0.16	
17.180	0.50	0.13	0.43	0.55	0.41	1.35	0.69	0.11	0.17	
18.860	0.51	0.13	0.44	0.55	0.43	1.39	0.70	0.12	0.17	
20.700	0.51	0.13	0.44	0.55	0.43	1.40	0.70	0.12	0.18	
22.730	0.50	0.13	0.43	0.53	0.43	1.36	0.68	0.13	0.17	
24.950	0.49	0.13	0.41	0.51	0.42	1.28	0.64	0.13	0.17	
27.380	0.47	0.12	0.39	0.49	0.40	1.21	0.59	0.13	0.16	
30.070	0.46	0.12	0.35	0.47	0.39	1.17	0.56	0.14	0.16	

Particle diameter ( $\mu\text{m}$ )	P2EJA-1	P2EJA-2	P2EJA-5	P2EJA-6	P2EJA-7	P2EJA-11	P2EJA-12	P2EJA-14	P2EJA-16	P2EJA-17
33.000	0.46	0.12	0.33	0.47	0.39	0.69	1.20	0.55	0.16	0.17
36.240	0.48	0.13	0.33	0.49	0.40	0.72	1.29	0.57	0.19	0.19
39.770	0.52	0.15	0.38	0.53	0.45	0.78	1.42	0.60	0.24	0.22
43.660	0.56	0.18	0.47	0.57	0.52	0.85	1.58	0.64	0.31	0.27
47.930	0.61	0.21	0.54	0.62	0.59	0.92	1.73	0.66	0.39	0.33
52.630	0.65	0.24	0.55	0.66	0.62	0.98	1.87	0.67	0.49	0.39
57.770	0.71	0.28	0.54	0.71	0.60	1.03	2.03	0.66	0.62	0.45
63.410	0.79	0.35	0.57	0.78	0.60	1.09	2.22	0.64	0.79	0.55
69.620	0.92	0.43	0.68	0.89	0.64	1.17	2.50	0.64	1.02	0.70
76.430	1.09	0.54	0.83	1.04	0.74	1.30	2.89	0.67	1.30	0.89
83.900	1.32	0.68	1.01	1.22	0.89	1.48	3.36	0.71	1.61	1.11
92.090	1.58	0.86	1.20	1.44	1.05	1.71	3.91	0.78	1.94	1.35
101.100	1.86	1.05	1.38	1.69	1.19	2.02	4.47	0.86	2.35	1.69
111.000	2.12	1.20	1.57	1.97	1.33	2.40	4.96	0.95	2.95	2.29
121.800	2.36	1.28	1.78	2.29	1.51	2.86	5.23	1.07	3.89	3.38
133.700	2.57	1.31	2.01	2.71	1.67	3.40	5.11	1.22	5.26	5.13
146.800	2.78	1.30	2.25	3.27	1.79	4.03	4.51	1.41	6.95	7.44
161.200	3.07	1.24	2.59	4.02	1.94	4.75	3.47	1.67	8.62	9.86
176.800	3.51	1.16	3.15	4.98	2.24	5.52	2.22	2.02	9.80	11.70
194.200	4.17	1.14	4.06	6.08	2.76	6.24	1.07	2.48	10.10	12.60
213.200	5.07	1.24	5.40	7.16	3.59	6.75	0.35	3.07	9.34	12.00
234.100	6.10	1.47	7.07	7.96	4.81	6.83	0.06	3.77	7.87	10.30
256.800	7.04	1.83	8.71	8.22	6.33	6.32	0.00	4.53	6.08	7.35
282.100	7.64	2.33	9.80	7.76	7.87	5.21	0.00	5.26	4.34	3.44
309.600	7.63	3.06	9.84	6.59	8.96	3.72	0.00	5.82	2.88	0.71
339.800	6.92	4.09	8.60	4.94	9.15	2.15	0.00	6.08	1.74	0.03
373.100	5.58	5.47	6.29	3.16	8.21	0.92	0.00	5.96	0.90	0.00
409.600	3.91	7.10	3.47	1.56	6.48	0.24	0.00	5.44	0.35	0.00
449.700	2.26	8.70	1.13	0.54	4.59	0.03	0.00	4.60	0.12	0.00
493.600	0.98	9.74	0.14	0.09	3.06	0.00	0.00	3.57	0.12	0.00
541.900	0.28	9.69	0.00	0.01	1.90	0.00	0.00	2.51	0.26	0.00
594.900	0.04	8.40	0.00	0.00	0.91	0.00	0.00	1.61	0.43	0.00
653.000	0.00	6.20	0.00	0.00	0.33	0.00	0.00	1.00	0.47	0.00
716.900	0.00	3.90	0.00	0.00	0.19	0.00	0.00	0.70	0.36	0.00
786.900	0.00	2.35	0.00	0.00	0.11	0.00	0.00	0.66	0.27	0.00
863.900	0.00	1.75	0.00	0.00	0.01	0.00	0.00	0.80	0.35	0.00
948.200	0.00	1.76	0.00	0.00	0.00	0.00	0.00	1.00	0.51	0.00
1041.000	0.00	1.72	0.00	0.00	0.00	0.00	0.00	1.09	0.48	0.00
1143.000	0.00	1.08	0.00	0.00	0.00	0.00	0.00	0.96	0.30	0.00
1255.000	0.00	0.28	0.00	0.00	0.00	0.00	0.00	0.60	0.11	0.00
1377.000	0.00	0.02	0.00	0.00	0.00	0.00	0.00	0.24	0.01	0.00
1512.000	0.00	0.00	0.00	0.00	0.00	0.00	0.00	0.05	0.00	0.00
1660.000	0.00	0.00	0.00	0.00	0.00	0.00	0.00	0.00	0.00	0.00
1822.000	0.00	0.00	0.00	0.00	0.00	0.00	0.00	0.00	0.00	0.00
2000.000	0.00	0.00	0.00	0.00	0.00	0.00	0.00	0.00	0.00	0.00

## Appendix A3

**Particle-size analysis of eight sandy samples (differential volume per cent).**

<b>Particle diameter (<math>\mu\text{m}</math>)</b>	<b>P2EJA-19</b>	<b>P2EJA-21</b>	<b>P2EJA-22</b>	<b>P2EJA-23</b>	<b>P2EJA-24</b>	<b>P2EJA-26</b>	<b>P2EJA-27</b>	<b>P2EJA-28</b>
0.412	0.02	0.01	0.02	0.02	0.02	0.01	0.01	0.08
0.452	0.04	0.02	0.04	0.04	0.03	0.02	0.03	0.14
0.496	0.06	0.03	0.06	0.06	0.04	0.03	0.05	0.20
0.545	0.09	0.05	0.09	0.09	0.06	0.04	0.06	0.29
0.598	0.11	0.06	0.11	0.11	0.08	0.05	0.08	0.35
0.657	0.13	0.07	0.13	0.13	0.09	0.06	0.10	0.41
0.721	0.15	0.08	0.15	0.15	0.11	0.07	0.11	0.45
0.791	0.17	0.09	0.18	0.17	0.12	0.08	0.13	0.49
0.869	0.19	0.10	0.19	0.19	0.14	0.09	0.14	0.52
0.953	0.20	0.11	0.21	0.21	0.15	0.09	0.16	0.54
1.047	0.22	0.11	0.23	0.22	0.16	0.10	0.17	0.55
1.149	0.23	0.12	0.24	0.24	0.18	0.11	0.18	0.56
1.261	0.25	0.12	0.26	0.25	0.19	0.12	0.19	0.56
1.385	0.26	0.12	0.27	0.27	0.20	0.12	0.19	0.57
1.520	0.27	0.13	0.28	0.28	0.21	0.13	0.20	0.58
1.669	0.29	0.13	0.29	0.29	0.22	0.14	0.21	0.59
1.832	0.31	0.13	0.30	0.30	0.24	0.15	0.21	0.61
2.010	0.32	0.13	0.32	0.32	0.25	0.15	0.22	0.63
2.207	0.34	0.13	0.33	0.33	0.26	0.16	0.22	0.66
2.423	0.36	0.13	0.34	0.35	0.27	0.16	0.23	0.70
2.660	0.39	0.14	0.35	0.36	0.28	0.17	0.23	0.73
2.920	0.41	0.14	0.36	0.38	0.30	0.18	0.24	0.77
3.206	0.44	0.15	0.38	0.40	0.31	0.19	0.25	0.81
3.519	0.47	0.15	0.39	0.42	0.32	0.19	0.26	0.85
3.862	0.49	0.16	0.40	0.44	0.34	0.20	0.27	0.89
4.241	0.52	0.16	0.42	0.46	0.35	0.21	0.28	0.93
4.656	0.55	0.17	0.43	0.48	0.36	0.22	0.29	0.96
5.111	0.58	0.18	0.44	0.50	0.38	0.22	0.31	0.99
5.611	0.60	0.18	0.46	0.52	0.39	0.23	0.32	1.02
6.158	0.63	0.18	0.47	0.54	0.40	0.24	0.32	1.04
6.761	0.65	0.19	0.47	0.55	0.42	0.24	0.33	1.06
7.421	0.67	0.19	0.48	0.57	0.43	0.25	0.33	1.07
8.147	0.69	0.19	0.48	0.58	0.44	0.25	0.34	1.08
8.944	0.71	0.19	0.49	0.60	0.45	0.25	0.34	1.09
9.819	0.73	0.18	0.49	0.61	0.47	0.25	0.34	1.09
10.780	0.75	0.18	0.49	0.63	0.48	0.25	0.34	1.10
11.830	0.77	0.18	0.49	0.64	0.49	0.25	0.34	1.11
12.990	0.79	0.18	0.49	0.66	0.51	0.25	0.35	1.13
14.260	0.82	0.19	0.49	0.69	0.53	0.26	0.37	1.16
15.650	0.85	0.20	0.50	0.72	0.55	0.27	0.39	1.22
17.180	0.88	0.21	0.51	0.75	0.58	0.28	0.42	1.28
18.860	0.90	0.22	0.52	0.78	0.60	0.29	0.45	1.33
20.700	0.92	0.23	0.51	0.80	0.62	0.30	0.47	1.33
22.730	0.91	0.23	0.50	0.80	0.62	0.29	0.47	1.29
24.950	0.89	0.23	0.47	0.78	0.62	0.28	0.47	1.21
27.380	0.86	0.23	0.44	0.76	0.62	0.26	0.46	1.12
30.070	0.85	0.23	0.42	0.74	0.62	0.24	0.45	1.06
33.000	0.86	0.25	0.42	0.74	0.63	0.23	0.47	1.05

Particle diameter ( $\mu\text{m}$ )	P2EJA-19	P2EJA-21	P2EJA-22	P2EJA-23	P2EJA-24	P2EJA-26	P2EJA-27	P2EJA-28
36.240	0.90	0.30	0.43	0.76	0.66	0.24	0.52	1.09
39.770	0.98	0.37	0.47	0.81	0.71	0.27	0.60	1.16
43.660	1.08	0.45	0.52	0.86	0.76	0.32	0.71	1.21
47.930	1.21	0.55	0.57	0.92	0.82	0.35	0.81	1.23
52.630	1.37	0.65	0.61	0.98	0.88	0.37	0.89	1.19
57.770	1.58	0.76	0.67	1.05	0.97	0.39	0.96	1.14
63.410	1.90	0.91	0.74	1.15	1.08	0.45	1.07	1.10
69.620	2.35	1.11	0.85	1.31	1.26	0.55	1.26	1.12
76.430	2.96	1.39	1.00	1.55	1.49	0.67	1.58	1.23
83.900	3.71	1.72	1.18	1.88	1.78	0.83	2.01	1.43
92.090	4.55	2.10	1.39	2.27	2.11	1.01	2.55	1.71
101.100	5.41	2.56	1.61	2.69	2.42	1.22	3.25	2.04
111.000	6.24	3.24	1.83	3.08	2.69	1.42	4.19	2.42
121.800	6.98	4.36	2.07	3.40	2.88	1.64	5.45	2.89
133.700	7.51	5.99	2.33	3.60	3.02	1.88	6.87	3.54
146.800	7.62	7.95	2.65	3.69	3.16	2.16	8.10	4.41
161.200	7.07	9.74	3.06	3.71	3.38	2.48	8.76	5.41
176.800	5.82	10.70	3.61	3.76	3.81	2.85	8.61	6.23
194.200	4.06	10.50	4.28	3.92	4.52	3.28	7.82	6.45
213.200	2.16	9.25	5.04	4.26	5.47	3.78	6.74	5.79
234.100	0.79	7.36	5.81	4.73	6.48	4.32	5.74	4.36
256.800	0.14	5.37	6.44	5.20	7.24	4.85	4.71	2.48
282.100	0.01	3.44	6.81	5.46	7.42	5.35	3.02	0.96
309.600	0.00	1.60	6.79	5.32	6.81	5.84	0.96	0.19
339.800	0.00	0.37	6.33	4.70	5.49	6.27	0.07	0.02
373.100	0.00	0.02	5.48	3.68	3.75	6.49	0.00	0.00
409.600	0.00	0.00	4.34	2.48	1.97	6.37	0.00	0.00
449.700	0.00	0.00	3.10	1.30	0.71	5.94	0.00	0.00
493.600	0.00	0.00	1.91	0.47	0.13	5.24	0.00	0.00
541.900	0.00	0.00	0.92	0.09	0.01	4.30	0.00	0.00
594.900	0.00	0.00	0.30	0.01	0.00	3.14	0.00	0.00
653.000	0.00	0.00	0.05	0.00	0.00	1.86	0.00	0.00
716.900	0.00	0.00	0.00	0.00	0.00	0.81	0.00	0.00
786.900	0.00	0.00	0.00	0.00	0.00	0.42	0.00	0.00
863.900	0.00	0.00	0.00	0.00	0.00	0.63	0.00	0.00
948.200	0.00	0.00	0.00	0.00	0.00	1.25	0.00	0.00
1041.000	0.00	0.00	0.00	0.00	0.00	1.45	0.00	0.00
1143.000	0.00	0.00	0.00	0.00	0.00	0.66	0.00	0.00
1255.000	0.00	0.00	0.00	0.00	0.00	0.06	0.00	0.00
1377.000	0.00	0.00	0.00	0.00	0.00	0.00	0.00	0.00
1512.000	0.00	0.00	0.00	0.00	0.00	0.00	0.00	0.00
1660.000	0.00	0.00	0.00	0.00	0.00	0.00	0.00	0.00
1822.000	0.00	0.00	0.00	0.00	0.00	0.00	0.00	0.00
2000.000	0.00	0.00	0.00	0.00	0.00	0.00	0.00	0.00